

# SCIENTIFIC REPORTS



OPEN

## Microprofiling of nitrogen patches in paddy soil: Analysis of spatiotemporal nutrient heterogeneity at the microscale

Yilin Li<sup>1</sup>, Herbert J. Kronzucker<sup>2</sup> & Weiming Shi<sup>1</sup>

Received: 06 November 2015

Accepted: 16 May 2016

Published: 06 June 2016

Flooded paddy soil ecosystems in the tropics support the cultivation of the majority of the world's leading crop, rice, and nitrogen (N) availability in the paddy-soil rooting zone limits rice production more than any other nutritional factor. Yet, little is known about the dynamic response of paddy soil to N-fertiliser application, in terms of horizontal and vertical patchiness in N distribution and transformation. Here, we present a microscale analysis of the profile of ammonium ( $\text{NH}_4^+$ ) and nitrate ( $\text{NO}_3^-$ ), nitrification, oxygen ( $\text{O}_{2\text{water}}$  and  $\text{O}_{2\text{soil}}$ ), and pH ( $\text{pH}_{\text{water}}$  and  $\text{pH}_{\text{soil}}$ ) in paddy soils, collected from two representative rice-production areas in subtropical China.  $\text{NH}_4^+$  and  $\text{NO}_3^-$  exhibited dramatic spatiotemporal profiles within N patches on the microscale. We show that  $\text{pH}_{\text{soil}}$  became constant at 1.0–3.5 mm depth, and  $\text{O}_{2\text{soil}}$  became undetectable at 1.7–4.0 mm. Fertiliser application significantly increased pH, and decreased  $\text{O}_2$ , within N patches. Path analysis showed that the factors governing nitrification scaled in the order:  $\text{pH}_{\text{water}} > \text{pH}_{\text{soil}} > \text{NH}_4^+ > \text{O}_{2\text{water}} > \text{NO}_3^- > \text{O}_{2\text{soil}}$ . We discuss the soil properties that decide the degree of nutrient patchiness within them and argue that such knowledge is critical to intelligent appraisals of nutrient-use efficiencies in the field.

It is now well established more generally that soil nutrients, including N, are distributed in a heterogeneous or patchy manner within ecosystems<sup>1,2</sup> due to a combination of natural and anthropogenic factors. In agricultural soils, N fertiliser application is the main anthropogenic driver that produces heterogeneity in soil N distribution, and fundamentally affects local N pools and N-cycling processes within soil<sup>3</sup>. Recent research on soil heterogeneity has almost exclusively focused on plant behavior. When roots encounter a nutrient-rich zone or patch, they often proliferate within it, including increases in elongation of individual roots<sup>4</sup>; total root length<sup>5</sup>; root production<sup>6</sup>; and extent of lateral branching<sup>7</sup>. These plastic responses by the root system have been proposed as the major mechanism employed by the root system to allow plants to cope with the heterogeneous supply of nutrients in soil<sup>1</sup>. Variations in both root biomass and N uptake rate per unit root biomass are important in contributing to the variations in the abilities of species to capture N from ephemeral patches<sup>8</sup>. Field studies have shown that plant roots respond most strongly to N given in pulses and least strongly to a continuous nutrient supply<sup>9</sup>. Furthermore, there was a positive relationship between N uptake rate, relative growth rate, and root system biomass<sup>8</sup>. In addition to the plastic responses of plant roots, there have been reports that soil N heterogeneity influences seedling recruitment<sup>10</sup>, vegetation succession<sup>11</sup>, plant species coexistence and competition<sup>12</sup>, and invasion of non-native plants into natural ecosystems<sup>13</sup>.

In flooded paddy soils, N is applied principally as ammonium ( $\text{NH}_4^+$ )-based or urea fertilisers<sup>14</sup>. The use of urea has increased rapidly in the past 40 years, and urea is now the most important N fertiliser in rice production throughout the world<sup>15</sup>. Instead of broadcast fertilisation, urea is frequently applied in a concentrated manner as basal manure, such as in hole applications, band and strip placements, in particular in paddy soils throughout China. One of the key advantages of these application methods is a reduction of N loss through nitrification-coupled denitrification<sup>16</sup> and ammonia ( $\text{NH}_3$ ) volatilisation<sup>17</sup>. When urea granules are applied into paddy soil in a concentrated manner, N patches establish rapidly, resulting in significant N heterogeneity in paddy

<sup>1</sup>State Key Laboratory of Soil and Sustainable Agriculture, Institute of Soil Science, Chinese Academy of Sciences, Nanjing 210008, PR China. <sup>2</sup>Department of Biological Sciences, University of Toronto, 1265 Military Trail, Toronto, Ontario, M1C 1A4, Canada. Correspondence and requests for materials should be addressed to W.S. (email: wmsi@issas.ac.cn)

soils, which are further accentuated by spatiotemporal fluctuations. The microzone around such intensively applied N fertiliser displays significant variations in ion concentrations, pH, chemical N transformation rates, and rice root behavior, which cannot be deduced from analysis of the bulk soil.

A paddy field has a complex three-dimensional structure within N patches that are formed by concentrated fertilisation. Naturally, when N fertiliser is applied, much higher N concentrations will be established at the fertilisation site and the surrounding microcosm than in unfertilised locations (i.e., the bulk soil), in particular during the time periods immediately following applications. Geostatistical descriptions of soil-N heterogeneity patterns for various ecosystems are abundant in the literature, but accounts on agricultural soils are rare<sup>2,8</sup>. Soil-N heterogeneity in association with N fertilisation using concentrated fertilisation in agricultural systems appears to be much more pronounced than that seen in natural ecosystem. Root proliferation into nutrient-rich zones or patches is considered by some as a foraging response to this heterogeneous nature of the nutrient environment, which depends on the growth rate of the plant, the geometry of the root system, and the size and strength of the patch encountered<sup>18</sup>. However, little is known about the extent to which N nutrient patches vary within themselves and the extent to which they impact surrounding soil and pivotal N-cycling processes such as nitrification.

Nitrification, which is performed by ammonia-oxidising bacteria (AOB)<sup>19</sup> or ammonia-oxidising archaea (AOA)<sup>20–23</sup> converting  $\text{NH}_4^+$  to nitrite ( $\text{NO}_2^-$ ), and then by nitrite-oxidising bacteria (NOB)<sup>24</sup> converting the latter to nitrate ( $\text{NO}_3^-$ ), is a key process in the global N cycle. Therefore, nitrification is critical to the supply of plant-available N in rice fields as well as to the overall balance of  $\text{NH}_4^+$  and  $\text{NO}_3^-$ <sup>25</sup>. Regardless of whether AOB, AOA, or NOB are all strict aerobic chemolithoautotrophic microorganisms, the microbial N transformations can only occur in the presence of oxygen ( $\text{O}_2$ ) and, thus, would be restricted to the upper few millimeters of flooded soils where  $\text{O}_2$  is measurable<sup>26</sup>. In our recent studies, the  $\text{O}_2$  dissolved in the rhizosphere soil was found to be significantly improved by radial  $\text{O}_2$  loss (ROL) from rice roots, promoting rhizospheric nitrification<sup>27</sup>. Duan *et al.*<sup>28</sup> and Zhao *et al.*<sup>29</sup> found that partial replacement of  $\text{NH}_4^+$  with  $\text{NO}_3^-$  could greatly improve the growth, yield, and N acquisition of rice. They speculated that the increased uptake of  $\text{NH}_4^+$  was promoted by  $\text{NO}_3^-$ . Clearly, the  $\text{NO}_3^-$  that is produced in nitrification at the root surface and within the rhizosphere in soils is very important for rice N nutrition<sup>30</sup>. The relationship between rhizosphere nitrification and NUE in rice was demonstrated in our previous study<sup>31</sup>.

N concentrations within fertiliser patches can be expected to be manifold higher than in the bulk soil. However, it remains unanswered what scale and magnitude such differences might assume in waterlogged paddy soils and how the spatial variations of  $\text{NH}_4^+$ ,  $\text{NO}_3^-$ , nitrification activity, pH,  $\text{O}_2$  and their temporal changes contribute to the spatial variation of the total inorganic N pool. In this study, two paddy soils were selected to examine these questions. The selected soils have the following characteristics: (1) they were collected from two representative rice production areas in subtropical China: Yingtan city, Jiangxi Province (YT paddy soil) and Qianjiang city, Hubei Province (QJ paddy soil); (2) YT paddy soil was derived from Quaternary red clay with a low overall pH value, and QJ paddy soil was derived from river alluvium with a high overall pH value; (3) both soils are subjected to similar fertility levels and tillage practices; (4) the average annual yields (obtained by double-cropping of rice) in Yingtan are significantly lower than those in Qianjiang. To obtain precise results for soil pH and  $\text{O}_2$ , microelectrodes were used in our experiments. Microelectrodes were produced with a small-enough tip diameter ( $\phi = 25 \mu\text{m}$ , Unisense, Aarhus, Denmark) to facilitate ready insertion into soil and plant tissues without damage, such as are routinely used in *in situ* measurements in plant physiology, environmental science, and related fields<sup>32</sup>. Hence, the present study was designed to measure and analyze, by path analysis (see methods), soil  $\text{NH}_4^+$ ,  $\text{NO}_3^-$ , pH, and  $\text{O}_2$  within N patches in paddy soils with the goal of substantially improving our understanding of the microbial nitrification process that is pivotal to rice N nutrition and of the factors that control it<sup>33</sup> within the heterogeneous reality of soil-N chemistry.

## Results

**Spatiotemporal fluctuations of ammonium and nitrate concentrations in nitrogen patches.** It was obvious that the  $\text{NH}_4^+$  concentrations strongly decreased with increasing distance from the N fertilisation site (Fig. 1). For example, the  $\text{NH}_4^+$ -N concentrations of YT and QJ at the fertilisation site were 2.66 and 3.92 times those measured at a distance of 40 mm away from the fertilisation site, at 7 d after fertilisation, respectively. The range of the N patch became more extensive with time, and disappeared at 40 d after urea application in both paddy soils (Fig. 1). The temporal variations of  $\text{NH}_4^+$  concentrations in N patches differed between the paddy soils derived from different parent material. The  $\text{NH}_4^+$  concentrations in the fertiliser patch of YT and QJ increased and decreased with incubation time, respectively, and became constant by 40 d following N application (Fig. 1), except for  $\text{NH}_4^+$  concentrations near the N-application sites in QJ paddy soil, which exhibited an initial increase followed by a decrease within 40 d after N application (Fig. 1). The  $\text{NH}_4^+$  concentrations at a far distance from the N-fertilisation site (>20 mm away) and those in control (CK) without fertiliser application, increased with time in both paddy soils within 40 d following N application (Supplementary Fig. S1). Both paddy soils differed significantly in  $\text{NH}_4^+$ -N concentrations, with an average of  $\sim 20 \text{ mg kg}^{-1}$  in YT soil and  $\sim 2 \text{ mg kg}^{-1}$  in QJ soil, respectively. Compared with CK, N fertilisation significantly increased the  $\text{NH}_4^+$  concentration in the paddy soil (Supplementary Fig. S1).

Compared with the spatiotemporal variations in  $\text{NH}_4^+$ , there were no significant spatiotemporal  $\text{NO}_3^-$  patch phenomena in the paddy soils tested (Fig. 2). When urea was applied to the waterlogged soils,  $\text{NO}_3^-$  concentrations showed almost no concentration gradients in terms of spatial distribution. The  $\text{NO}_3^-$  concentrations in the N-application sites at the beginning of N fertilisation (1 d after fertilisation in YT soil) were significantly lower than those in controls without fertilisation (Fig. 2). The  $\text{NO}_3^-$  concentrations decreased with time, while the pattern of decrease differed between the two paddy soils. The  $\text{NO}_3^-$  concentration in YT paddy soil peaked at 1 d after N fertilisation, then decreased slightly at 3 d after N fertilisation, and became stable at 5 d after N fertilisation (Fig. 2). The  $\text{NO}_3^-$  concentration in QJ paddy soil showed a gradual decline during the incubation period (Fig. 2).

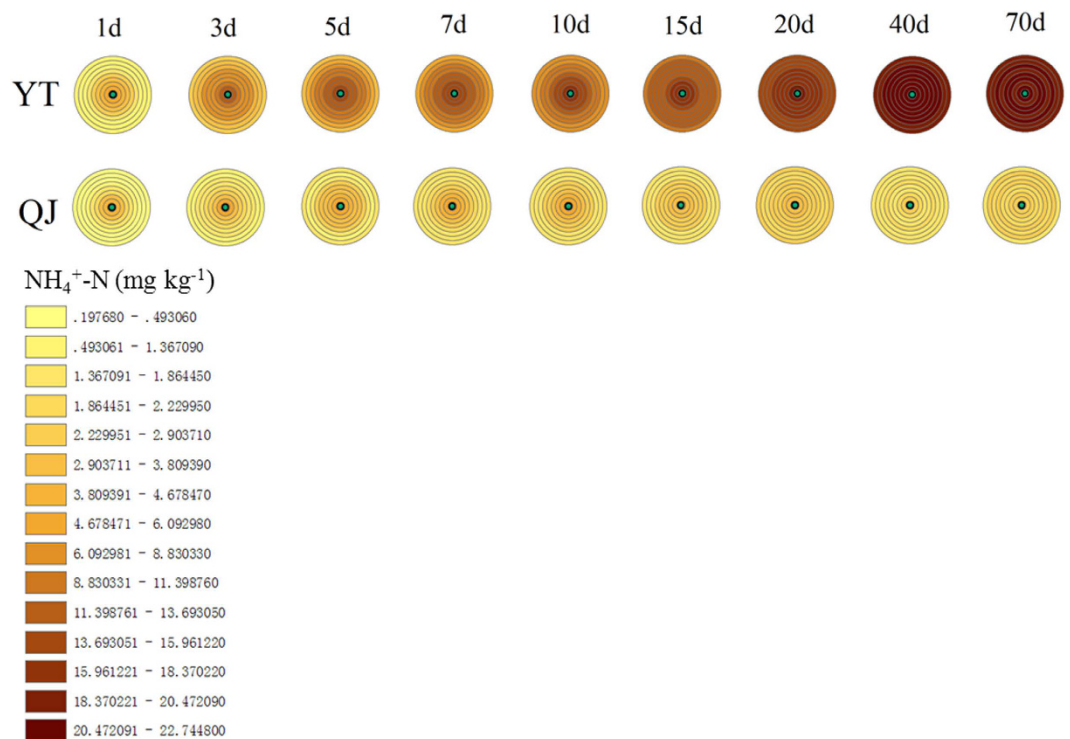


**Figure 1. Distribution of NH<sub>4</sub><sup>+</sup> concentrations in Yingtan (YT) and Qianjiang (QJ) paddy soils.** The concentric circles in the upper row represent YT paddy soil, and the concentric circles in the row below represent QJ paddy soil. The concentrations measured at different distance from the fertilisation site (the circles in the concentric circles, from inside to out, represent 0, 2, 4, 6, 8, 10, 20, 30 and 40 mm distance from the fertilisation zone, respectively) at different sampling dates (the concentric circles left-to-right represent 1, 3, 5, 7, 10, 15, 20, 40 and 70 days after fertilisation, respectively). Mean values are shown for a sample size of three replicates.

The maximal NO<sub>3</sub><sup>-</sup> concentration of the QJ was significantly higher than that measured in the YT soil (Fig. 2), which might be due to the higher nitrification activity in QJ than in YT soil (Fig. 3). N fertilisation increased the NO<sub>3</sub><sup>-</sup> concentration in YT soil (Supplementary Fig. S2). Within 7 d after N fertilisation, there was no significant effect of N fertilisation on the increase in NO<sub>3</sub><sup>-</sup> concentration, while the pattern of increase became obvious after that period in the QJ treatment (Supplementary Fig. S2).

**Spatiotemporal fluctuations in nitrification activity in nitrogen patches.** Fertiliser patch phenomena for nitrification were significant in paddy soil derived from red soil (YT), while they seemed not obvious in paddy soil derived from river alluvium (QJ). Nitrification activities within the N patches were significantly higher than those in the bulk soil, and they decreased with distance from the fertilisation site in YT soil, (Fig. 3), while there was no difference among the various sites sampled in QJ soil (Fig. 3). In YT soil, N-patch nitrification activity and patch range increased slowly over time during the first 7 d, and a rate of 0.05 mg kg<sup>-1</sup> h<sup>-1</sup> was maintained during the period of 40 d after fertilisation, after which the N-patch effect disappeared, at 70 d after fertilisation (Fig. 3). The nitrification activity measured in QJ soil showed almost no variance with time, with values of ~8.5 mg kg<sup>-1</sup> h<sup>-1</sup> during the first 40 d, but decreased significantly at the last sampling time (Fig. 3). An unexpected observation was that the nitrification activity measured in QJ soil was nearly 200 times that measured in the YT soil. Compared to control, N fertilisation significantly increased soil nitrification (Supplementary Fig. S3).

**Spatial pH fluctuations in nitrogen patches.** The pH values measured in the water layer slightly decreased with horizontal distance from the fertilisation sites in both soil types, while those in YT were much lower than in QJ, with ~5.5 and 8.3, respectively (Fig. 4). When the microelectrode tip touched the water-soil interface, the pH value measured increased sharply in YT soil, while declining sharply in QJ soil. pH values varied greatly with soil depth initially but became constant at 1.0–3.5 mm depth, approaching neutrality (Fig. 4). Soil pH values decreased with distance from the fertilisation sites, and pH values measured in the water layer and in soil in the CK were significantly lower than those in the fertilisation treatments, indicating that urea fertilisation can enhance the water-layer and soil pH in waterlogged paddy soil by about 0.5 to 1 pH units. Urea fertilisation seemed to impact soil pH more significantly in paddy soil derived from red soil (YT) than in paddy soil derived from river alluvium (QJ), i.e. the fertiliser patch phenomenon vis-à-vis soil pH is more pronounced in paddy soil derived from red soil. Overall, soil pH values were higher in QJ than in YT (Fig. 4). For example, pH values were 6.4 and 7.6 at a depth of 0.5 mm from the soil surface, and 6.5 and 7.2 at a depth of 5 mm in the YT and QJ, respectively (Fig. 4).

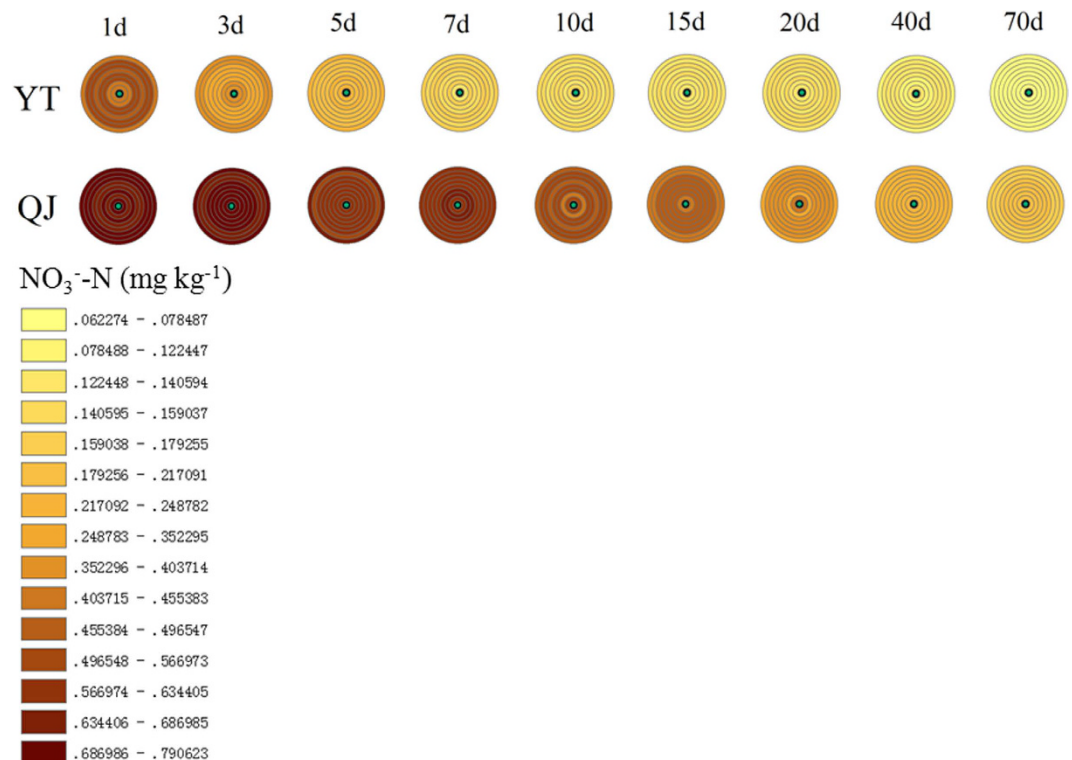


**Figure 2. Distribution of NO<sub>3</sub><sup>-</sup> concentrations in Yingtan (YT) and Qianjiang (QJ) paddy soils.** The concentric circles in the upper row represent YT paddy soil, and the concentric circles in the row below represent QJ paddy soil. The concentrations measured at different distance from the fertilisation site (the circles in the concentric circles, from inside to out, represent 0, 2, 4, 6, 8, 10, 20, 30 and 40 mm distance from the fertilisation zone, respectively) at different sampling dates (the concentric circles left-to-right represent 1, 3, 5, 7, 10, 15, 20, 40 and 70 days after fertilisation, respectively). Mean values are shown for a sample size of three replicates.

**Spatial fluctuations in oxygen concentration in nitrogen patches.** Oxygen dissolved in the water layer remained constant near 220 and 244  $\mu\text{mol L}^{-1}$  in the YT and QJ soils, respectively (Fig. 5). O<sub>2</sub> concentration declined sharply in the water-soil interface to 5–10% compared with that in the water layer. With increasing soil depth, O<sub>2</sub> concentrations decreased rapidly and smoothly and became undetectable within 1.7–4.0 mm depth below the soil surface (Fig. 5). The soil depth at which dissolved O<sub>2</sub> concentration became undetectable showed a ranking of QJ > YT, and that depth was greater in controls than in fertilisation treatments. The O<sub>2</sub> concentration in the fertilisation sites, when assessed horizontally, consistently showed minimal levels and increased with distance away from the fertilisation sites in both treatments, and the CK showed maximal O<sub>2</sub> concentrations compared to the fertilisation treatments. Urea fertilisation decreased the soil O<sub>2</sub> concentration by about 50% compared with CK (Fig. 5). The O<sub>2</sub> concentrations in both water layers and in soil ranked QJ > YT.

**Major soil properties affecting nitrification activity.** Simple correlation coefficients ( $r$ ) between NH<sub>4</sub><sup>+</sup>, NO<sub>3</sub><sup>-</sup>, pH<sub>water</sub> (water pH), pH<sub>soil</sub> (soil pH), O<sub>2water</sub> (water O<sub>2</sub>) and O<sub>2soil</sub> (soil O<sub>2</sub>) are presented for comparison with path analysis results. The uncorrelated residual value ( $U$ ) was low (0.077), while the coefficient of determination ( $R^2$ ) was high (0.994), indicating that the path analysis model could explain the majority (99.4%) of variation in soil nitrification (Table 1). Path analysis partitioned each  $r$  value into one direct effect and five indirect effects. Partitioning by path analysis showed significant direct effects by pH<sub>water</sub> ( $P_{37} = 1.234$ ,  $p < 0.001$ ) and pH<sub>soil</sub> ( $P_{37} = -0.154$ ,  $p < 0.001$ ) on nitrification. Furthermore, the direct effects of NH<sub>4</sub><sup>+</sup>, NO<sub>3</sub><sup>-</sup>, O<sub>2water</sub> and O<sub>2soil</sub> on nitrification were not significant ( $p > 0.05$ ), while the simple correlation analysis revealed that NH<sub>4</sub><sup>+</sup>, NO<sub>3</sub><sup>-</sup>, pH<sub>water</sub>, pH<sub>soil</sub>, O<sub>2water</sub> and O<sub>2soil</sub> were all significantly correlated with nitrification ( $p < 0.001$ ). Examination by path analysis revealed that pH<sub>water</sub> had negative indirect path coefficients through NH<sub>4</sub><sup>+</sup> ( $r_{13P37} = -1.220$ ,  $p < 0.001$ ), while it had positive indirect path coefficients through NO<sub>3</sub><sup>-</sup> ( $r_{23P37} = 1.196$ ,  $p < 0.001$ ), pH<sub>soil</sub> ( $r_{34P37} = 1.141$ ,  $p < 0.001$ ), O<sub>2water</sub> ( $r_{35P37} = 1.183$ ,  $p < 0.001$ ), and O<sub>2soil</sub> ( $r_{36P37} = 1.098$ ,  $p < 0.001$ ).

## Discussion

Ammonium derived from the mineralisation of organic matter is transformed into NO<sub>3</sub><sup>-</sup> through the nitrification process. Both ions are presented in variable concentrations in different ecosystems, and frequently plants show preferences for one N form or another<sup>34,35</sup>. The fate over time of NH<sub>4</sub><sup>+</sup> and NO<sub>3</sub><sup>-</sup> concentrations

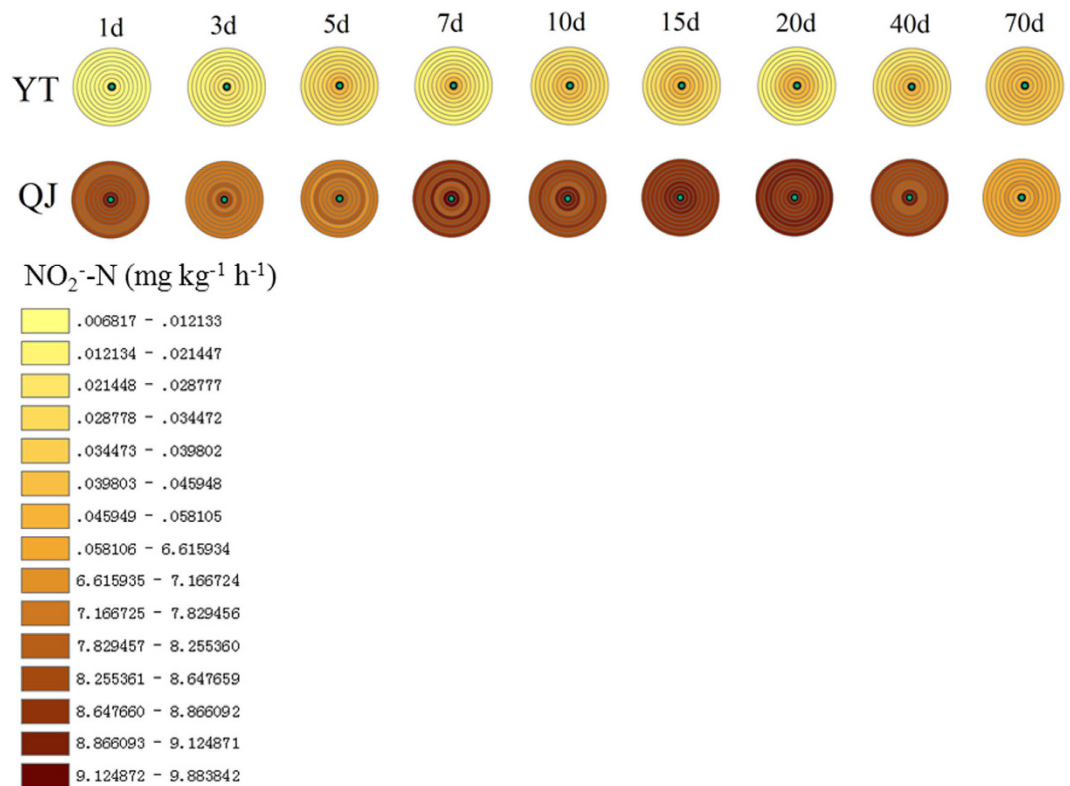


**Figure 3. Distribution of short-term nitrification activity in Yingtan (YT) and Qianjiang (QJ) paddy soils.** The concentric circles in the upper row represent YT paddy soil, and the concentric circles in the row below represent QJ paddy soil. The nitrification activities measured at different distance from the fertilisation site (the circles in the concentric diagrams, from inside to out, represent 0, 2, 4, 6, 8, 10, 20, 30 and 40 mm away from the fertilisation zone, respectively) at different sampling dates (the concentric circles left-to-right represent 1, 3, 5, 7, 10, 15, 20, 40 and 70 days after fertilisation, respectively). Mean values are shown for a sample size of three replicates.

in N patches in agricultural soils such as paddies had not been hitherto examined. Dramatic such changes were seen in our study, although the different origin and behavior of the two N sources in soils will influence spatial distribution<sup>12</sup> (Figs 1 and 2).

In the paddy soils in our study,  $\text{NH}_4^+$  was generated by urea hydrolysis, with additional contributions from soil organic N. Consequently,  $\text{NH}_4^+$  concentrations inside the N patch were significantly higher than those in the bulk soil or in unfertilised soil (Fig. 1, Supplementary Fig. S1).  $\text{NH}_4^+$  concentrations decreased with increasing distance from the N fertilisation site, and the range of the  $\text{NH}_4^+$ -N patch increased over time (Fig. 1). This result supports the notion that transport of  $\text{NH}_4^+$  in soil occurs mainly by diffusion<sup>33</sup>. A large fraction of organic N was present in both paddy soils at the start of the experiment (see Methods). Because farming practices on the two paddy fields from which the soils derived are characterised by long-term inorganic and organic fertilisation in the rice season and manure application in the fallow (winter) season (reclamation greater than 50 years). The process of mineralisation of the organic N pool is an important contributor to the generation of inorganic N in the soil<sup>31</sup>. A comparison between the treatments and the controls allowed for calculations that revealed that less than 30% of  $\text{NH}_4^+$  accumulated in the N patch derived from mineralisation before 10 d after fertilisation. Certainly the proportion of mineralised  $\text{NH}_4^+$  increased with time. At the preliminary stage of fertilisation,  $\text{NH}_4^+$  accumulation resulting from mineralisation accounted for a much smaller percentage. For example, the proportions of  $\text{NH}_4^+$  derived from mineralisation were only about 3.5% at 1 d after fertilisation. Paddy soils collected from Taihu Region, one of the most ancient rice cultivation areas of China, were studied with 120-day anaerobic incubation at 25 and 35 °C without rice planting, and the organic N mineralisation ranged from 4.0% to 9.4% of total N (60–241  $\text{mg kg}^{-1}$ )<sup>36</sup>. Thus,  $\text{NH}_4^+$  generation from organic N in both paddy soil types may be expected to be high. However,  $\text{NH}_4^+$  concentrations in QJ were much lower than in YT (except in the fertilisation zone on the 1st day following fertilisation; see Fig. 1). Ammonium ions, loosely bound to water molecules, predominate in water at a pH value above 7.2. With increasing hydroxyl-ion concentrations in the water, ionised  $\text{NH}_4^+$  increasingly converts to nonionised  $\text{NH}_3$ , which increases the risk of  $\text{NH}_3$  volatilisation<sup>37</sup>. Because the pH values tested both in the water layer and soil of QJ were all higher than in YT, and the pH in the water layer was above 8.0 (Fig. 4). Therefore,  $\text{NH}_3$  generated from  $\text{NH}_4^+$  in QJ paddy soil was volatilised more intensely. The unexpectedly high nitrification activities measured in the QJ paddy soil (more than 200 times those seen in the YT paddy soil, see Fig. 3) might lead to large quantities of  $\text{NH}_4^+$  consumption as nitrification substrate, further accentuating  $\text{NH}_4^+$  depletion (Fig. 1).

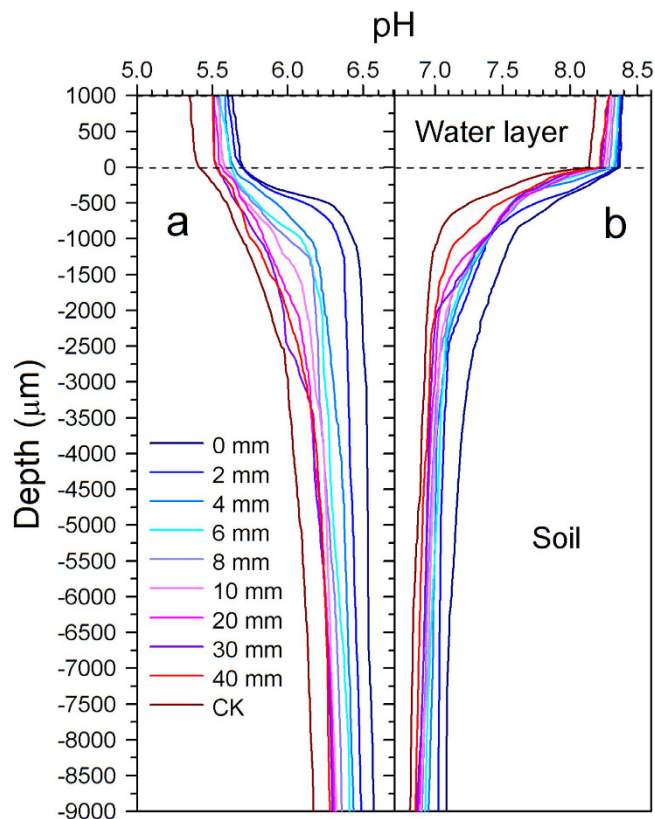


**Figure 4.** pH profiles in (a) Yingtan (YT) and (b) Qianjiang (QJ) paddy soils measured at different distances from the fertilisation site at 40 d after fertilisation. A 25- $\mu\text{m}$ -diameter pH microelectrode was used (pH 25, Unisense, Aarhus, Denmark). CK, without N fertilisation. The ordinate represents the depth of the water layer (0–1,000  $\mu\text{m}$ ) and soil (0–9,000  $\mu\text{m}$ ), and the tick label of “0” shows the water–soil interface. The pH profile was determined in the right and left compartments of each box and in the center at different distances from the nylon nets in each treatment. Profile results in repeats were so similar that a representative result is shown.

In contrast to most agricultural soils, where  $\text{NO}_3^-$  is the predominant N form, the flooded conditions in paddy soil greatly restrain the microbial formation of  $\text{NO}_3^-$ , and therefore  $\text{NH}_4^+$  is the main form of N available to young rice plants<sup>38</sup>. Indeed,  $\text{NO}_3^-$  concentrations measured in both soils in our study were two orders of magnitude lower than  $\text{NH}_4^+$  concentrations (Figs 1 and 2). The  $\text{NO}_3^-$  diffusion rate in flooded lowland soils has been determined to be 1.33  $\text{cm}^2 \text{day}^{-1}$ , which is approximately 7 times faster than  $\text{NH}_4^+$  diffusion<sup>39</sup>. Therefore, diffusion is expected to play a more important role for  $\text{NO}_3^-$  distribution in flooded paddy soil than for that of  $\text{NH}_4^+$ , which is relatively even (Fig. 2). Since  $\text{NO}_3^-$  is an anion, not significantly adsorbed by soil colloids, it tends to diffuse rapidly to other parts of the soil, unlike  $\text{NH}_4^+$ , which is readily adsorbed by negatively charged soil colloids. However,  $\text{NO}_3^-$  dynamics in association with  $\text{NO}_3^-$ -N patches are more complex. Despite nitrification, nitrifier denitrification<sup>40</sup> (the pathway of nitrification in which  $\text{NH}_3$  is oxidised to  $\text{NO}_2^-$  followed by the reduction of  $\text{NO}_2^-$  to nitric oxide (NO), nitrous oxide ( $\text{N}_2\text{O}$ ), and molecular nitrogen ( $\text{N}_2$ )) and  $\text{NO}_3^-$  reduction to  $\text{NH}_4^+$  (DNRA)<sup>41</sup> would also influence spatiotemporal dynamics of  $\text{NO}_3^-$  in paddy soils. We also note that, in our experiment, the observed  $\text{NO}_3^-$  decreases and  $\text{NH}_4^+$  accumulation in the YT soil over time (Figs 1 and 2), could also be attributable to DNRA.

Given the stoichiometry of nitrification, 2 mol of  $\text{O}_2$  and 1 mol of  $\text{NH}_4^+$  are consumed per 1 mol of  $\text{NO}_3^-$  formed<sup>42</sup>. Once formed,  $\text{NO}_3^-$  may diffuse down into the reduced soil where it can be denitrified<sup>43</sup>.  $\text{O}_2$  and  $\text{NH}_4^+$  depletion over time, and denitrification activity in the more anaerobic soil strata, all led to a decrease of  $\text{NO}_3^-$  concentrations with time (Fig. 2), even though nitrification activities themselves in both soils did not show distinct decreases over time (Fig. 3). Because rice roots can efficiently absorb  $\text{NO}_3^-$ <sup>44</sup>, the denitrification substrate is accordingly removed rapidly in the field, reducing denitrification in the rhizosphere. In some sense, therefore, rice planting can decrease N loss by denitrification compared to fallow soil. Paddy soil without rice, such as examined in our study, would increase the risk of denitrification, and accordingly decrease the  $\text{NO}_3^-$  dissolved in the paddy soil. Using the multiple ring buffer graphics in our experiments, the spatiotemporal fluctuations of soil  $\text{NH}_4^+$  and  $\text{NO}_3^-$  concentrations within N patches could be shown intuitively (Figs 1 and 2). Also, the pattern of growth and decline in nitrification activity within N patches was well visualised (Fig. 3) by using this kind of graphic, and is presented here for the first time.

Unlike in other ecosystems, paddy soil is deficient in dissolved  $\text{O}_2$  because of the agricultural practice of regular flooding. The  $\text{O}_2$  is detected only in a millimeter-thick surface layer, leaving the bulk soil anoxic, restricting the activity of nitrifying microorganisms to this small zone<sup>33</sup>. The available  $\text{O}_2$  in flooded paddy soil is mainly derived

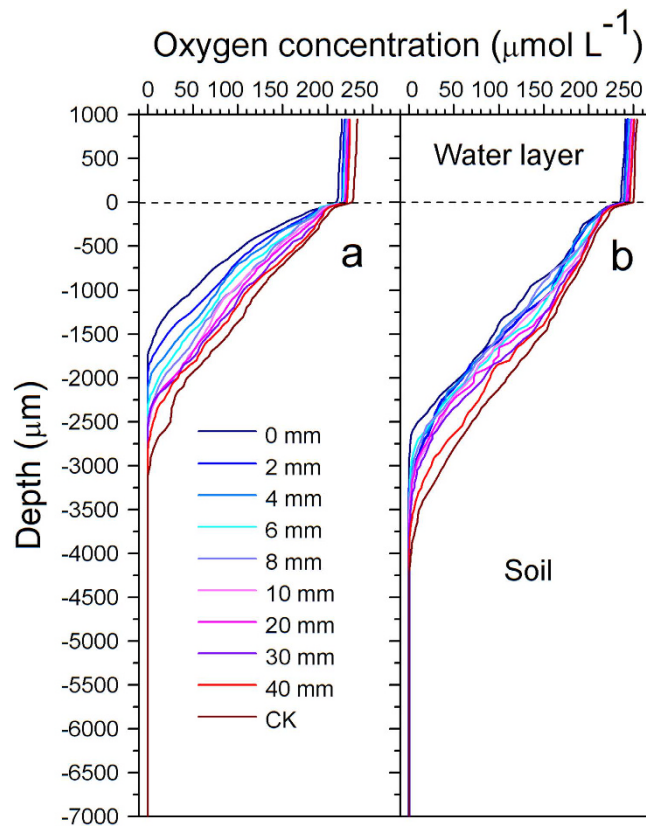


**Figure 5.** Oxygen concentration profiles in (a) Yingtan (YT) and (b) Qianjiang (QJ) paddy soils measured at different distances from the fertilisation site at 40 d after fertilisation. A 25- $\mu\text{m}$ -diameter  $\text{O}_2$  microelectrode was used (OXY25, Unisense, Aarhus, Denmark). CK, without N fertilisation. The ordinate represents the depth of the water layer (0–1,000  $\mu\text{m}$ ) and soil (0–7,000  $\mu\text{m}$ ), and the tick label of “0” shows the water-soil interface. The  $\text{O}_2$  profile was determined in the right and left compartments of each box and in the center at different distances from the nylon nets in each treatment. Profile results in repeats were so similar that a representative result is shown.

Variable	$\text{NH}_4^+$	$\text{NO}_3^-$	$\text{pH}_{\text{water}}$	$\text{pH}_{\text{soil}}$	$\text{O}_{2\text{water}}$	$\text{O}_{2\text{soil}}$	$r$	$R^2$	$U$
$\text{NH}_4^+$	<i>0.111</i>	0.025	-1.220	0.135	-0.030	-0.009	-0.988***	0.994***	0.077
$\text{NO}_3^-$	-0.107	<i>-0.026</i>	1.196	-0.137	0.029	0.009	0.964***		
$\text{pH}_{\text{water}}$	-0.110	-0.025	<i>1.234***</i>	-0.142	0.030	0.009	0.995***		
$\text{pH}_{\text{soil}}$	-0.098	-0.023	1.141	<i>-0.154***</i>	0.026	0.007	0.900***		
$\text{O}_{2\text{water}}$	-0.108	-0.025	1.183	-0.130	<i>0.031</i>	0.010	0.961***		
$\text{O}_{2\text{soil}}$	-0.103	-0.023	1.098	-0.113	0.030	<i>0.010</i>	0.900***		

**Table 1.** Direct effects (diagonal, *italics*) and indirect effects (off diagonal) of soil properties on nitrification.  $\text{NH}_4^+$  ( $\text{NH}_4^+$  dissolved in soil);  $\text{NO}_3^-$  ( $\text{NO}_3^-$  dissolved in soil);  $\text{pH}_{\text{water}}$  (pH value measured in the water layer);  $\text{pH}_{\text{soil}}$  (pH value measured in the soil profile);  $\text{O}_{2\text{water}}$  ( $\text{O}_2$  concentration measured in the water layer) and  $\text{O}_{2\text{soil}}$  ( $\text{O}_2$  concentration measured in the soil profile). \*\*\*significant at the level of  $p < 0.001$ , \*\*significant at the level of  $p < 0.01$ , \*significant at the level of  $p < 0.05$ .

from the micro-amounts of  $\text{O}_2$  dissolved in the soil and the  $\text{O}_2$  from irrigation water, and is enhanced only immediately within the rice rhizosphere by root-directed  $\text{O}_2$  transport and exudation through rice aerenchyma tissue<sup>42</sup>. In our study, although the N patch seemed to be dissolved by 40 d following urea application in both paddy soils (Fig. 1),  $\text{O}_2$  concentrations and pH still revealed different horizontal distribution characteristics between the N-patch area and the bulk soil (Figs 4 and 5).

Urea fertilisation could increase the water-layer and soil pH in waterlogged paddy fields by about 0.5–1 pH units (Fig. 4). Urea fertilisation seemed to produce a more significant change in soil pH in acid paddy soil (YT) than in alkaline paddy soil (QJ). Volatilisation losses can occur from acid as well as alkaline soils due to high pH and  $\text{NH}_4^+$  enrichment at the microsite where urea granules dissolve and hydrolyze. Acidification of the fertiliser microsite is a mechanism by which  $\text{NH}_3$  volatilisation may be reduced<sup>45</sup>. In our experiment, *in situ* results showed that pH became constant at  $\sim 1.0$ – $3.5$  mm depth below the soil surface and approached neutrality in both soils

Property	YT	QJ
pH (water:soil, 2.5:1)	5.02	8.05
Organic matter (g kg <sup>-1</sup> )	39.1	27.3
Total N (g kg <sup>-1</sup> )	1.74	1.49
C/N ratio	13.0	10.6
NH <sub>4</sub> <sup>+</sup> -N (mg kg <sup>-1</sup> )	2.27	1.46
NO <sub>3</sub> <sup>-</sup> -N (mg kg <sup>-1</sup> )	0.21	0.48
Clay (%)	20.9	12.7
Locality	Yingtian, Jiangxi prov.	Qianjiang, Hubei prov.
Reclamation year	>50	>50
Parent material	Quaternary red clay	River alluvium
Average yield of double cropping rice per year (kg ha <sup>-1</sup> )	10,000	12,500

**Table 2. Properties of the two paddy soils used in the study.** Fertilisation strategy was in concentrated applications on both soils (see Methods).

tested (Fig. 4). However, these results might be different if rice planting were to occur. The pH of rice paddy soils following two weeks of flooding usually ranges from 6.5–7.0, although some reports have shown pH to remain as low as 5.0 or as high as 8.0<sup>45</sup>. Fortunately, the rice root system (mainly composed of adventitious root at this stage of development) tends to be concentrated in 0–5-cm depth in paddy soil<sup>27</sup>, i.e. in the neutral-pH zone, which allows rice roots to avoid damage from relatively high or low pH. Like pH, O<sub>2</sub> concentration also showed fertiliser-patch phenomena. Urea fertilisation decreased the soil O<sub>2</sub> concentration to about 50% compared with the unfertilised treatment at 40 d after fertilisation in the waterlogged condition (Fig. 5). Aerobic processes such as nitrification are intensified within the N patch, leading to soil oxygen depletion there.

The availabilities of NH<sub>4</sub><sup>+</sup> and O<sub>2</sub> are key factors determining the rate of nitrification<sup>25</sup>. Although the NH<sub>4</sub><sup>+</sup> concentration in the QJ paddy soil was significantly lower than in the YT soil, the relatively higher pH (Fig. 4) and O<sub>2</sub> concentration (Fig. 5) promoted nitrification (Fig. 3). Due to the higher amounts of O<sub>2</sub> consumed in the degradation of organic matter and in the oxidation of reduced compounds<sup>46</sup>, YT soil displayed more severe O<sub>2</sub> depletion, given its higher organic matter content (see Methods). In addition, YT soil had relatively lower porosity (because of its higher clay content, see Methods), which led to less O<sub>2</sub> dissolution (Fig. 5).

Natural factors, such as soil parent materials, topography, climate, as well as human factors, such as reclamation time and history of fertilisation, are all important factors influencing the soil-formation process in paddy soils<sup>47</sup>. Due to differences in soil formation, soil properties vary considerably among soil types<sup>48</sup>, and these, in turn, influence soil N-transformation processes, in particular nitrification and denitrification. However, soil properties are often strongly interrelated, making it challenging to establish a causal relationship between soil properties and nitrification activity if a simple correlation analysis is used. By contrast, path analysis is a statistical technique that distinguishes correlation and causation by partitioning correlation into direct and indirect effects<sup>49</sup>. The direct effect represents the direct contribution of a predictor variable (e.g., soil properties) to a response variable (e.g., nitrification activity). The indirect effect represents the contribution of a predictor variable to a response variable via another predictor variable. Therefore, path analysis can provide insight into the relative contribution of causal relationships and the direction of a causal path. Path analysis has been used extensively in agronomic studies, such as in examining the relationships between soil properties and phosphorus sorption capacity<sup>50</sup> or the adsorption of heavy metals<sup>51</sup>. However, to the best of our knowledge, path analysis has not been hitherto employed to examine the relationships between soil properties and nitrification activity.

In our experiments, soil O<sub>2</sub> concentration and pH might be the principal factors affecting nitrification as nitrification substrate was not limiting, and the manifestations of these determinants were different between the soil types. Path analysis confirmed the main contribution by pH, especially water-layer pH, which played the most significant role ( $P_{37} = 1.234$ ,  $p < 0.001$ ) in nitrification, and the second contributor was soil pH ( $P_{37} = -0.154$ ,  $p < 0.001$ ; see Table 2). Although simple correlation analysis revealed that O<sub>2</sub> dissolved in the water layer and soil were both significantly correlated with nitrification ( $p < 0.001$ ), path analysis revealed the correlation mainly derived from the strong effect of water-layer pH on O<sub>2</sub> dissolved in the water layer ( $r_{35P37} = 1.183$ ,  $p < 0.001$ ) and the soil profile ( $r_{36P37} = 1.098$ ,  $p < 0.001$ ; Table 2); path analysis partitions correlations into direct and indirect effects and distinguishes between correlation and causation<sup>49</sup>. It should be noted that the use of mean values for O<sub>2</sub> measured in identical vertical profiles, necessitated by the limitations in the soil slice collection method, might lead to small underestimations of nitrification rates, as the penetration depth of O<sub>2</sub> into the soil strongly affects nitrification and is typically limited to the uppermost few millimeters of soil. However, as the same procedure was applied throughout, we posit that the data between our treatments are directly comparable, and the correlations and trends observed hold even though a finer resolution for soil sample collection was not technically feasible.

Generally speaking, N patches derived from concentrated fertilisation shows a dramatically changing spatio-temporal pattern in paddy-soil environments, and nitrification displays colourful performance at different stages. The rice plant once planted into paddy soil is expected to affect the nitrification process, while its behavior, in turn, would be greatly affected by the patch. Although the results obtained from fallow soil are not in themselves sufficient to understand the behavior of the paddy field situation that includes the rice crop, and a diverse mesofauna and macrofauna, study of the simplified soil system represents an important first step and is essential to the understanding of the detailed behavior of nitrification within N patches on account of soil properties.



Poising N-fertiliser applications efficiently and without negative environmental consequences will require a thorough understanding of patch phenomena in agricultural soils. The dynamics within N patches in paddy soil in the presence of rice should be the subject of dedicated future research efforts.

## Methods

**Description of the paddy soil collected sites.** The paddy soils were collected from two representative rice production areas in subtropical China, Yingtan city (YT paddy soil, 28°15'20" N, 116°55'30" E), Jiangxi Province and Qianjiang city (QJ paddy soil, 30° 15' 36" N, 112° 31' 48" E), Hubei Province. The detailed properties of both paddy soils are shown in Table 2.

**Soil incubation and sampling.** An organic glass incubation box was divided into three compartments with two nylon nets (30 µm mesh size) where fertiliser-soil mixture was placed in the middle of the box and soil without fertiliser was in the two side compartments. The mesh of the nylon net was fine enough to allow penetration of water and nutrient elements. Design and specifications of this incubation box were as displayed in the rhizobox diagram<sup>14</sup> (detail of the incubation box see Supplementary Fig. S4).

Each incubation box was filled with 600 g of paddy soil (air-dried, ground and sieved through 0.85 mm, which explicitly excludes soil mesofauna and macrofauna). In the middle compartment, 100 g soil was mixed thoroughly with urea (equivalent to 120 mg N kg<sup>-1</sup>) and KH<sub>2</sub>PO<sub>4</sub> (93 mg kg<sup>-1</sup>). The two side compartments were simultaneously filled with 250 g soil without fertiliser. For control (CK) experiments, boxes were filled with 600 g paddy soil without urea but with KH<sub>2</sub>PO<sub>4</sub> (93 mg kg<sup>-1</sup>) in the middle compartment. A depth of 1 cm of surface water was maintained by adding deionised water every morning and evening throughout the experimental period. All boxes were incubated in a constant incubator at 25 °C and with a 16 h photoperiod.

To avoid water layer interference with the chemical determinations, paddy soils were not watered in the evening of the day prior to the sampling date, to maintain a thin (1–2 mm) water layer. The advantage of this approach is that the soil is easy to slice and NO<sub>3</sub><sup>-</sup> concentrations can be determined more effectively. However, the disadvantage of this approach is that it imperceptibly stimulates nitrification and results in overestimates of the soil NO<sub>3</sub><sup>-</sup> concentration. Each sampling occurred at 7:00 am, and each treatment sample was kept in –20 °C for 2 h to rigidify the paddy soil for subsequent slicing; soil samples were then collected at distances of 0, 2, 4, 6, 8, 10, 20, 30 and 40 mm distance from the fertilisation zone, respectively, without vertical profiles (unlike the *in-situ* measurement of soil pH and O<sub>2</sub> concentration), for logistical reasons, although vertical redox gradients in submerged soils are also expected to influence the distribution of NH<sub>4</sub><sup>+</sup> and NO<sub>3</sub><sup>-</sup><sup>43</sup>. The soil samples collected from the right and left compartments at an identical horizontal distance were mixed together for the assessments of mineral N and nitrification activity at 1, 3, 5, 7, 10, 15, 20, 40 and 70 days after fertilisation, with three replicates.

**Mineral N assay.** Fresh soil samples were extracted with 2 mol l<sup>-1</sup> KCl (soil: solution ratio 1:10), and extracts were measured for NH<sub>4</sub><sup>+</sup> and NO<sub>3</sub><sup>-</sup> by a continuous-flow auto-analyzer (model Autoanalyzer 3, Bran + Luebbe, Hamburg, Germany). In the preliminary experiment, NO<sub>3</sub><sup>-</sup> concentration in flooded soil was so low as to be undetectable using the original extracts. Thus, subsequently, extracts were concentrated 10 times prior to determination.

**Short-term nitrification activity assay.** Short-term estimations are usually used in assays of nitrification activity. The principle is based on the determination of NO<sub>2</sub><sup>-</sup> after the incubation of soil samples with NaClO<sub>3</sub> (an inhibitor of NO<sub>2</sub><sup>-</sup> oxidation) in the absence of NH<sub>4</sub><sup>+</sup> for 24 h at 25 °C<sup>52</sup>. The procedure is briefly described as follows. Each soil sample (5 g of moist soil) was shaken with 2.5 mL of NaClO<sub>3</sub> (75 mmol L<sup>-1</sup>) at 170 rpm on a rotary shaker for 30 min and then incubated for a further 24 h at 25 °C in order to prevent NO<sub>2</sub><sup>-</sup> conversion into NO<sub>3</sub><sup>-</sup>. After incubation, NO<sub>2</sub><sup>-</sup> was extracted from soil samples into a total volume of 15 mL using two solutions (first, 5 mL deionised H<sub>2</sub>O, and then 10 mL of 2 mol L<sup>-1</sup> KCl) by shaking at a 170 rpm speed for 30 min on a rotary shaker as described earlier. The contents were mixed thoroughly and immediately filtered. Five mL of the clear filtrate was pipetted into glass test tubes, followed by 3 mL of buffer (0.19 mol L<sup>-1</sup> NH<sub>4</sub>Cl, pH 8.5) and 2 mL of the reagent (dissolve 2 g of sulphanilamide and 0.1 g naphthyl-diethylene-diammonium chloride in 150 ml distilled water and 20 ml phosphoric acid were added. After cooling, dilution to 200 ml with distilled water) for NO<sub>2</sub><sup>-</sup> determination. The contents were again vigorously shaken and allowed to stand for 15 min at room temperature. Finally, the colour intensity was measured at 520 nm. For control measurements, soil samples were extracted as previously described after incubation with NaClO<sub>3</sub> at –20 °C. The determination was repeated three times using four incubation boxes (three for the samples and one for the control). Pre-experiments using the paddy soil tested (waterlogged for 40 d) to monitor the kinetics of NH<sub>3</sub> oxidation in the first 24 hours were performed, showing that NO<sub>2</sub><sup>-</sup> was produced linearly over time (p < 0.05). Short-term nitrification activity was expressed as the production of NO<sub>2</sub><sup>-</sup>-N per unit time and calculated according to equation (1):

$$\text{NO}_2^- \text{-N} = (\text{NO}_2^- \text{-N}_{\text{filtrate}} - \text{NO}_2^- \text{-N}_{\text{control}}) \times v / (W \times \text{dwt} \times h) \quad (1)$$

where NO<sub>2</sub><sup>-</sup>-N is the production of NO<sub>2</sub><sup>-</sup>-N per unit time (mg kg<sup>-1</sup> h<sup>-1</sup>), NO<sub>2</sub><sup>-</sup>-N<sub>filtrate</sub> is the determination of NO<sub>2</sub><sup>-</sup>-N after the incubation of soil samples with NaClO<sub>3</sub> for 24 h at 25 °C (mg l<sup>-1</sup>), NO<sub>2</sub><sup>-</sup>-N<sub>control</sub> is the determination of NO<sub>2</sub><sup>-</sup>-N after the incubation of soil samples with NaClO<sub>3</sub> for 24 h at –20 °C (mg l<sup>-1</sup>), dwt is the dry weight of 1 g moist soil used, W is the weight of the soil used (g), v is the total volume of solutions added to soil sample in the assay (ml), t is the incubation time (h).

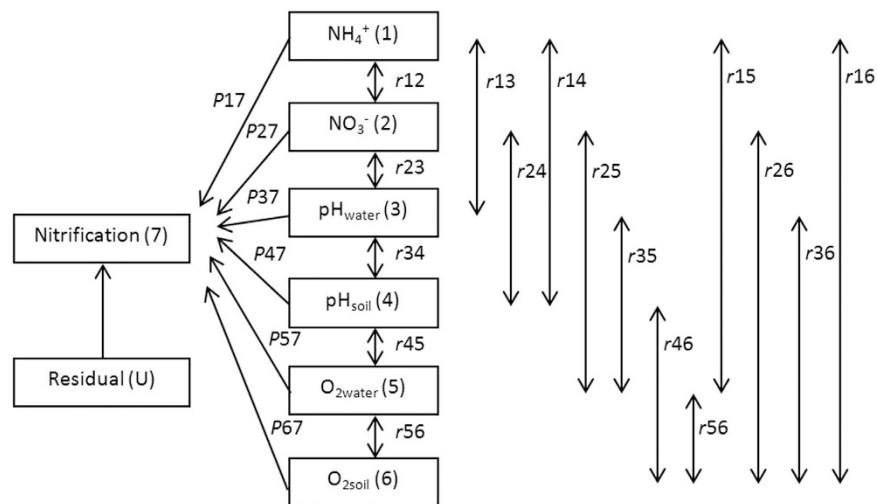


**Figure 6.** Path analysis diagram for the relationship between nitrification and soil properties. Path coefficients ( $P_{ij}$ ) of soil properties are represented by single-headed arrows while simple correlation coefficients ( $r_{ij}$ ) between variables are represented by double-headed arrows. Subscript designations for soil properties are identified numerically as follows: 1,  $\text{NH}_4^+$  dissolved in soil ( $\text{NH}_4^+$ ); 2,  $\text{NO}_3^-$  dissolved in soil ( $\text{NO}_3^-$ ); 3, pH value measured in the water layer ( $\text{pH}_{\text{water}}$ ); 4, pH value measured in the soil profile ( $\text{pH}_{\text{soil}}$ ); 5,  $\text{O}_2$  concentration measured in the water layer ( $\text{O}_{2\text{water}}$ ) and 6,  $\text{O}_2$  concentration measured in the soil profile ( $\text{O}_{2\text{soil}}$ ).

***In situ* measurement of soil pH and oxygen concentrations.** Incubation boxes, in three replicates, were also used for the *in-situ* measurement of soil pH and  $\text{O}_2$  concentrations at 40 d after fertilisation. The incubation condition was as described above, except that in boxes for *in-situ* measurements, a water layer of 1 cm was always maintained.

The pH microelectrode was a miniaturised pH glass electrode with an outer tip diameter of  $25\ \mu\text{m}$ <sup>53</sup> (pH 25, Unisense, Aarhus, Denmark). The  $\text{O}_2$  microelectrode was also a miniaturised Clark-type  $\text{O}_2$  electrode with a guard cathode<sup>54</sup> (OXY25,  $\phi = 25\ \mu\text{m}$ , Unisense, Aarhus, Denmark). The tips of both pH and  $\text{O}_2$  microelectrodes were highly fragile, so a micromanipulator (MM33-2, Unisense) with a motor controller (MC-232, Unisense) were used, with the micromanipulator fixed on the lab stand (LS18, Unisense) to avoid disturbance during the microelectrode movement. As measurements of pH values and  $\text{O}_2$  concentrations were very sensitive to the temperature, a thermometer was used to monitor soil temperature during the measurement. Both measurements for pH and  $\text{O}_2$  were conducted at  $50\text{-}\mu\text{m}$  depth intervals, and the periods for “wait before measure” and “measure” were both set to 3 s. All the *in situ* measurements were performed in a zero-electrical-noise-interference laboratory, at  $25^\circ\text{C}$ .

**Data analysis.** All statistical analyses were performed using SPSS version 13.0, and one-way ANOVA with a homogeneity of variance test was performed, followed by an LSD test to check for quantitative differences between treatments.  $P < 0.05$  was set as the significance cut-off.

Path analysis was used to evaluate the relationships between nitrification and soil properties, including  $\text{NH}_4^+$ ,  $\text{NO}_3^-$ ,  $\text{pH}_{\text{water}}$  (water pH),  $\text{pH}_{\text{soil}}$  (soil pH),  $\text{O}_{2\text{water}}$  (water  $\text{O}_2$ ) and  $\text{O}_{2\text{soil}}$  (soil  $\text{O}_2$ ). Because  $\text{NH}_4^+$ ,  $\text{NO}_3^-$ , and nitrification were measured at 1, 3, 5, 7, 10, 15, 20, 40 and 70 days after fertilisation, respectively, without vertical determination, and  $\text{O}_2$  and pH were only measured at 40 d after fertilisation, the data for  $\text{NH}_4^+$ ,  $\text{NO}_3^-$ , and nitrification at 40 d after fertilisation, as well as the mean values of the data of  $\text{O}_2$  and pH measured in the identical vertical profile (separated as water layer and soil vertical-profiles), were used for the path analyses. The direct effects of soil properties on nitrification are represented by single-headed arrows while coefficients of intercorrelation between soil properties are represented by double-headed arrows in Fig. 6. The direct effects of soil properties on nitrification are termed path coefficients and are standardised partial regression coefficients for each of the soil properties in the multiple linear regression against nitrification<sup>55</sup>. Indirect effects of soil properties on nitrification were calculated from the product of the simple correlation coefficient between soil properties and the path coefficient<sup>56</sup>. The correlation between nitrification and soil properties is the sum of the direct and indirect coefficients. In addition, an uncorrelated residue (U) was calculated for the model using the following equation (2):

$$U = \sqrt{1 - R^2} \quad (2)$$

where  $R^2$  is the coefficient of determination in the multiple regression equation between nitrification and the six soil properties. Path analysis results were determined as described in the following equations:

$$r_{17} = P_{17} + r_{12}P_{27} + r_{13}P_{37} + r_{14}P_{47} + r_{15}P_{57} + r_{16}P_{67} \quad (3)$$

$$r_{27} = r_{12}P_{17} + P_{27} + r_{23}P_{37} + r_{24}P_{47} + r_{25}P_{57} + r_{26}P_{67} \quad (4)$$

$$r_{37} = r_{13}P_{17} + r_{23}P_{27} + P_{37} + r_{34}P_{47} + r_{35}P_{57} + r_{36}P_{67} \quad (5)$$

$$r_{47} = r_{14}P_{17} + r_{24}P_{27} + r_{34}P_{37} + P_{47} + r_{45}P_{57} + r_{46}P_{67} \quad (6)$$

$$r_{57} = r_{15}P_{17} + r_{25}P_{27} + r_{35}P_{37} + r_{45}P_{47} + P_{57} + r_{56}P_{67} \quad (7)$$

$$r_{67} = r_{16}P_{17} + r_{26}P_{27} + r_{36}P_{37} + r_{46}P_{47} + r_{56}P_{57} + P_{67} \quad (8)$$

where  $r_{ij}$  is the simple correlation coefficient between nitrification and a soil property,  $P_{ij}$  is the path coefficient between nitrification and a soil property, and  $r_{ij}P_{ij}$  is the indirect effect of a soil property on nitrification. Subscript designations are: 1,  $\text{NH}_4^+$ ; 2,  $\text{NO}_3^-$ ; 3,  $\text{pH}_{\text{water}}$ ; 4,  $\text{pH}_{\text{soil}}$ ; 5,  $\text{O}_{2\text{water}}$ ; and 6,  $\text{O}_{2\text{soil}}$ . SPSS version 13.0 was used for statistical analysis.

## References

- Hodge, A. The plastic plant: root responses to heterogeneous supplies of nutrients. *New Phytol.* **162**, 9–24 (2004).
- Wang, L., Mou, P. P., Huang, J. & Wang, J. Spatial heterogeneity of soil nitrogen in a subtropical forest in China. *Plant Soil* **295**, 137–150 (2007).
- Pérez, C. A., Hedin, L. O. & Armesto, J. J. Nitrogen mineralization in two unpolluted old-growth forests of contrasting biodiversity and dynamics. *Ecosystems* **1**, 361–373 (1998).
- Zhang, H., Jennings, A., Barlow, P. W. & Forde, B. G. Dual pathways for regulation of root branching by nitrate. *PNAS* **96**, 6529–6534 (1999).
- Hodge, A., Robinson, D., Griffiths, B. S. & Fitter, A. H. Why plants bother: root proliferation results in increased nitrogen capture from an organic patch when two grasses compete. *Plant Cell Environ.* **22**, 811–820 (1999).
- Pregitzer, K. S., Hendrick, R. L. & Fogel, R. The demography of fine roots in response to patches of water and nitrogen. *New Phytol.* **125**, 575–580 (1993).
- Farley, R. A. & Fitter, A. H. The response of seven co-occurring woodland herbaceous perennials to localized nutrient-rich patches. *J. Ecol.* **87**, 849–859 (1999).
- James, J. J., Mangold, J. M., Sheley, R. L. & Svejcar, T. Root plasticity of native and invasive Great Basin species in response to soil nitrogen heterogeneity. *Range. Ecol. Manag.* **202**, 211–220 (2009).
- Moar, S. E. L. & Wilson, S. D. Root responses to nutrient patches in grassland and forest. *Plant Ecol.* **184**, 157–162 (2006).
- Mou, P., Fahey, T. J. & Hughes, J. W. Nutrient accumulation in vegetation following whole-tree harvest of a northern hardwood ecosystem. *J. Appl. Ecol.* **30**, 661–675 (1993).
- Gross, K. L., Pregitzer, K. S. & Burton, A. J. Spatial variation in nitrogen availability in three successional plant communities. *J. Ecol.* **83**, 357–367 (1995).
- Gallardo, A., Paramá, R. & Covelo, F. Difference between soil ammonium and nitrate spatial pattern in six plant communities. Simulated effect on plant populations. *Plant Soil* **279**, 333–346 (2006).
- Siemann, E. & Rogers, W. E. Changes in light and nitrogen availability under pioneer trees may indirectly facilitate tree invasions of grasslands. *J. Ecol.* **91**, 923–931 (2003).
- Li, Y. L., Zhang, Y. L., Hu, J. & Shen, Q. R. Contribution of Nitrification Happened in Rhizospheric Soil Growing with Different Rice Cultivars to N Nutrition. *Biol. Fert. Soils* **43**, 417–425 (2007).
- Bremner, J. M. Recent research on problems in the use of urea as a nitrogen fertilizer. *Fert. Res.* **42**, 321–329 (1995).
- Cai, Z. Ammonium transformation in paddy soils affected by the presence of nitrate. *Nutr. Cycl. Agroecosys.* **63**, 267–274 (2002).
- Gaudin, R. & Dupuy, J. Ammoniacal nutrition of transplanted rice fertilized with large urea granules. *Agron. J.* **91**, 33–36 (1999).
- Hutchings, M. J. & de Kroon, H. Foraging in plants: the role of morphological plasticity in resource acquisition. *Adv. Ecol. Res.* **25**, 159–238 (1994).
- Abbasi, M. K. & Adams, W. A. Loss of nitrogen in compacted grassland soil by simultaneous nitrification and denitrification. *Plant Soil* **200**, 265–277 (1998).
- Francis, C. A., Roberts, K. J., Beman, J. M., Santoro, A. E. & Oakley, B. B. Ubiquity and diversity of ammonia-oxidizing archaea in water columns and sediments of the ocean. *PNAS* **102**, 14683–14688 (2005).
- Venter, J. C. *et al.* Environmental genome shotgun sequencing of the Sargasso Sea. *Science* **304**, 66–74 (2004).
- Könneke, M. *et al.* Isolation of an autotrophic ammonia-oxidizing marine archaeon. *Nature* **437**, 543–546 (2005).
- Leininger, S. *et al.* Archaea predominate among ammonia-oxidizing prokaryotes in soils. *Nature* **442**, 806–809 (2006).
- Zhao, J., Wang, B. Z. & Jia, Z. J. Phylogenetically distinct phylotypes modulate nitrification in a paddy soil. *AEM* **81**, 3218–3227 (2015).
- Briones, A. M. *et al.* Influence of different cultivars on populations of ammonia-oxidizing bacteria in the root environment of rice. *AEM* **68**, 3067–3075 (2002).
- Chen, X. P., Zhu, Y. G., Xia, Y., Shen, J. P. & He, J. Z. Ammonia-oxidizing archaea: important players in paddy rhizosphere soil? *Environ. Microbiol.* **10**, 1978–1987 (2008).
- Li, Y. L., Shi, W. M. & Wang, X. X. New insights into how increases in fertility improve the growth of rice at the seedling stage in red soil regions of subtropical China. *PLOS ONE* **9**, e109161, doi: 10.1371/journal.pone.0109161 (2014).
- Duan, Y. H. *et al.* Responses of rice cultivars with different nitrogen use efficiency to partial replaced nitrate nutrition. *Ann. Bot.* **99**, 1153–1160 (2007).
- Zhao, X. Q., Zhao, S. P. & Shi, W. M. Enhancement of  $\text{NH}_4^+$  uptake by  $\text{NO}_3^-$  in relation to expression of nitrate-induced genes in rice (*Oryza sativa*) roots. *Pedosphere* **18**, 86–91 (2008).
- Kronzucker, H. J., Glass, A. D. M., Siddiqi, M. Y. & Kirk, G. J. D. Comparative kinetic analysis of ammonium and nitrate acquisition by tropical lowland rice: implications for rice cultivation and yield potential. *New Phytol.* **145**, 471–476 (2000).
- Li, Y. L., Fan, X. R. & Shen, Q. R. The relationship between rhizosphere nitrification and nitrogen-use efficiency in rice plants. *Plant Cell Environ.* **31**, 73–85 (2008).
- Pedersen, O., Rich, S. M. & Colmer, T. D. Surviving floods: leaf gas films improve  $\text{O}_2$  and  $\text{CO}_2$  exchange, root aeration, and growth of completely submerged rice. *Plant J.* **58**, 147–156 (2009).
- Arth, I. & Frenzel, P. Nitrification and denitrification in the rhizosphere of rice: the detection of processes by a new multi-channel electrode. *Biol. Fert. Soils* **31**, 427–435 (2000).

34. Kronzucker, H. J., Siddiqi, M. Y. & Glass, A. D. M. Conifer root discrimination against soil nitrate and the ecology of forest succession. *Nature*. **385**, 59–61 (1997).
35. Britto, D. T. & Kronzucker H. J. Ecological significance and complexity of N-source preference in plants. *Ann. Bot.* **112**, 957–963 (2013).
36. Li, H. L., Han, Y. & Cai, Z. C. Nitrogen mineralization in paddy soils of the Taihu region of China under anaerobic conditions: dynamics and model fitting. *Geoderma* **115**, 161–175 (2003).
37. Mikkelsen, D. S., De Datta, S. K. & Obcemea, W. N. Ammonia volatilization losses from flooded rice soils. *Soil Sci. Soc. Am. J.* **42**, 725–730 (1978).
38. Kronzucker, H. J. *et al.* Dynamic interactions between root  $\text{NH}_4^+$  influx and long-distance N translocation in rice: insights into feedback processes. *Plant Cell Physiol.* **39**, 1287–1293 (1998).
39. Reddy, K. R. & Patrick Jr, W. H. Denitrification losses in flooded rice fields. *Fert. Res.* **9**, 99–116 (1986).
40. Wrage, N., Velthof, G. L., van Beusichem, M. L. & Oenema, O. Role of nitrifier denitrification in the production of nitrous oxide. *Soil Biol. Biochem.* **33**, 1723–1732 (2001).
41. Lu, W. W. *et al.* *In situ* dissimilatory nitrate reduction to ammonium in a paddy soil fertilized with liquid cattle waste. *Pedosphere* **22**, 314–321 (2012).
42. Kirk, G. D. J. & Kronzucker, H. J. The potential for nitrification and nitrate uptake in the rhizosphere of wetland plants: a modelling study. *Ann. Bot.* **96**, 639–646 (2005).
43. Wells, N. S., Clough, T. J., Johnson-Beebout, S. E. & Buresh, R. J. Land management between crops affects soil inorganic nitrogen balance in a tropical rice system. *Nutr. Cycl. Agroecosyst.* **100**, 315–332 (2014).
44. Kronzucker, H. J., Siddiqi, M. Y., Glass, A. D. M. & Kirk, G. J. D. Nitrate-ammonium synergism in rice: a subcellular flux analysis. *Plant Physiol.* **119**, 1041–1046 (1999).
45. Fan, M. X. & Mackenzie, A. F. Urea and phosphate interactions in fertilizer microsites: ammonia volatilization and pH changes. *Soil Sci. Soc. Am. J.* **57**, 839–845 (1993).
46. Ratering, S. & Schnell, S. Nitrate-dependent iron (II) oxidation in paddy soil. *Environ. Microbiol.* **3**, 100–109 (2001).
47. Yuan, F., Ran, W., Shen, Q. R. & Wang, D. Z. Characterization of nitrifying bacteria communities of soils from different ecological regions of China by molecular and conventional methods. *Biol. Fert. Soils* **41**, 22–27 (2005).
48. Yan, X., Wang, D. J., Zhang, H. L., Zhang, G. & Wei, Z. Q. Organic amendments affect phosphorus sorption characteristics in a paddy soil. *Agr. Ecosyst. Environ.* **175**, 47–53 (2013).
49. Wright, S. The method of path coefficients. *Ann. Mat. Stat.* **5**, 161–215 (1934).
50. Kang, J., Hesterberg, D. & Osmond, D. L. Soil organic matter effects on phosphorus sorption: a path analysis. *Soil Sci. Soc. Am. J.* **73**, 360–366 (2008).
51. Ding, C. F., Zhang, T. L., Li, X. G. & Wang, X. X. Major controlling factors and prediction models for mercury transfer from soil to carrot. *J. Soil Sediment* **14**, 1136–1146 (2014).
52. Berg, P. & Rosswall, T. Ammonium oxidizer numbers, potential and actual oxidation rates in two Swedish arable soils. *Biol. Fert. Soils* **1**, 131–140 (1985).
53. Revsbech, N. P. & Jørgensen, B. B. Microelectrodes: their use in microbial ecology. *Adv. Microb. Ecol.* **9**, 293–352 (1986).
54. Revsbech, N. P. An oxygen microelectrode with a guard cathode. *Limnol. and Oceanogr.* **34**, 472–476 (1989).
55. Basta, N. T., Pantone, D. J. & Tabatabai, M. A. Path analysis of heavy metal adsorption by soil. *Agron. J.* **85**, 1054–1057 (1993).
56. Williams, W. A., Jones, M. B. & Demment, M. W. A concisetable for path analysis. *Agron. J.* **82**, 1022–1024 (1990).

## Acknowledgements

This research was financially supported by the Strategic Priority Research Program (B) of the Chinese Academy of Sciences (No. XDB15030100), the National Natural Science Foundation of China (No. 31471948), and the Knowledge Innovation Program of the Chinese Academy of Sciences (No. ISSASIP1608).

## Author Contributions

Y.L. and W.S. conceived the experiment, Y.L. conducted the experiments and Y.L., W.S. and H.J.K. analysed the results. W.S. provided advice on the experiment. Y.L., W.S. and H.J.K. wrote the paper. All authors reviewed the manuscript.

## Additional Information

**Supplementary information** accompanies this paper at <http://www.nature.com/srep>

**Competing financial interests:** The authors declare no competing financial interests.

**How to cite this article:** Li, Y. *et al.* Microprofiling of nitrogen patches in paddy soil: Analysis of spatiotemporal nutrient heterogeneity at the microscale. *Sci. Rep.* **6**, 27064; doi: 10.1038/srep27064 (2016).



This work is licensed under a Creative Commons Attribution 4.0 International License. The images or other third party material in this article are included in the article's Creative Commons license, unless indicated otherwise in the credit line; if the material is not included under the Creative Commons license, users will need to obtain permission from the license holder to reproduce the material. To view a copy of this license, visit <http://creativecommons.org/licenses/by/4.0/>